Published in final edited form as:
Ultrason Imaging. 2008 July ; 30(3): 189–200.

Noninvasive and Transient Blood-Brain Barrier Opening in the Hippocampus of Alzheimer's Double Transgenic Mice Using Focused Ultrasound

James J. Choi[1], **Shougang Wang**[2], **Truman R. Brown**[1,2], **Scott A. Small**[3], **Karen E. K. Duff**[4], and **Elisa E. Konofagou**[1,2]

[1]Department of Biomedical Engineering, Columbia University New York, NY 10027

[2]Department of Radiology, Columbia University New York, NY 10027

[3]Department of Neurology, Columbia University New York, NY 10027

[4]Department of Pathology, Columbia University New York, NY 10027

Abstract

The spatio-temporal nature of focused ultrasound-induced blood-brain barrier (BBB) opening as a brain drug delivery method was investigated in Alzheimer's disease model mice. The left hippocampus of transgenic (APP/PS1, $n = 3$) and nontransgenic ($n = 3$) mice was sonicated (frequency: 1.525 MHz, peak-negative pressure: 600 kPa, pulse length: 20 ms, duty cycle: 20%, duration: 1 min) *in vivo*, through their intact skin and skull, after intravenous injection of microbubbles (SonoVue®; 25 μl). Sequential, high-field MR images (9.4 Tesla) were acquired before and after injection of gadolinium (Omniscan™; 0.75 ml, molecular weight: 573.7 Da) on two separate days for each mouse. Gadolinium deposits through the ultrasound-induced BBB opening in the left hippocampus revealed significant contrast-enhancement in the MRI. On the following day, MRI revealed significant BBB closure within the same region. However, the BBB opening extent and BBB closing timeline varied in different regions within the same sonicated location. This indicates that opening and closing were dependent on the brain region targeted. No significant difference in BBB opening or closing behaviors was observed between the APP/PS1 and the nontransgenic mice. In conclusion, a BBB-impermeable molecule was noninvasively, transiently and reproducibly delivered to the hippocampus of Alzheimer's APP/PS1 mice.

Keywords

Alzheimer disease; blood-brain barrier; drug delivery system; magnetic resonance imaging; ultrasonic therapy

BACKGROUND

Alzheimer's disease (AD) is a progressive neurodegenerative disease that begins at the hippocampus and spreads to the remaining brain as the disease progresses. It is mainly characterized by the presence of extracellular amyloid plaques and intracellular neurofibrillary tangles in the brain. Cleavage of the amyloid precursor protein by β-secretase and γ-secretase leads to the aggregation of amyloid-β (Aβ) peptides, which constitute the core of the plaques. The current belief is that the accumulation of Aβ is the primary cause of

ek2191@columbia.edu.

AD and thus targeting it would be the best therapeutic approach. AD has affected 15.3 million people worldwide in 2000 and is expected to affect 63 million by 2030.1 Treating AD is therefore one of the most urgent medical needs in neurotherapeutics and, while current drugs improve associated symptoms, they do not induce profound disease-modifying effects.

The current standard of care for mild to moderate AD includes acetylcholinesterase inhibitors (AChEIs) and memantine.2 These compounds have been shown to be safe and have symptomatic benefits,3, 4 but no associated disease-modifying effects have been proven and patient benefits have been limited. As a result, new treatments are being developed including drugs that block Aβ aggregation, anti-amyloid immunotherapy and methods to modulate Aβ production (i.e., β-secretase and γ-secretase inhibitors). Many of the proposed methods involve molecules that are either too large (>400 Da) to traverse the blood-brain barrier (BBB) or incapable of localization to specific regions of the brain.5 For example, β-secretase inhibitors and modulators have shown great potential in reducing Aβ peptide levels6 without the undesirable off-target effects of γ-secretase inhibitors.7 In spite of their potential, β-secretase inhibitors are of limited use, since they are typically on the order of 1 kDa and, therefore, are BBB-impermeable. As a result, there is a great need for localized delivery of large, neurologically-potent drugs trans-BBB. The BBB constitutes thus the rate-limiting factor in brain drug delivery development for not only AD, but also neurological diseases in general.5

The BBB is the selective permeability barrier of the cerebral capillaries that protects the brain from harmful compounds and regulates its microenvironment.8 However, these properties are also the major impediments to successful neuropharmaceutical treatment. While many brain drug delivery methods are being developed to increase the trans-BBB deposition of agents, most do not encompass the necessary noninvasive, transient and localized characteristics of a successful technique.9 To our knowledge, the only method encompassing these characteristics is BBB opening with focused ultrasound (FUS).10

FUS localizes ultrasound energy to a millimeter-sized focal region defined as the sonicated area, which is affected by the ultrasound beam while the surrounding regions remain relatively unaffected. In a recent case report of a human transcranial Doppler sonography study using low-frequency ultrasound (300 kHz) for diagnostic purposes, unexpected extravasations of an MRI contrast agent due to BBB disruption was observed in the patient. 11 This technique was previously optimized by intravenously (IV) injecting pre-formed gas-filled microbubbles prior to sonication. The stimulation of bubble activity by the ultrasound induced transient BBB opening. This effect was demonstrated in rabbits,10, 12 mice13-19 and rats20 with a variety of compounds being trans-BBB delivered: gadolinium-based MRI contrast agents,10, 17, 18 Evans Blue,13 Herceptin,13 doxorubicin,20 and fluorescent dextrans at different molecular weights (3 and 70 kDa).21 However, to our knowledge, there has been no study that characterizes the FUS-induced trans-BBB distribution of agents and the closing timeline in a neurodegenerative disease animal model.

In this study, the effects of age and the presence of disease on the FUS-induced BBB opening and closure in transgenic APP/PS1 mice is addressed and compared to the effects in nontransgenic (NTg) mice. Analysis of the BBB opening was performed *in vivo* using a high-field MRI system with high in-plane spatial resolution for monitoring the slow permeation of gadolinium and temporal analysis of drug deposition.17, 18 The feasibility of BBB opening in transgenic AD mice is demonstrated, thus laying the foundations for future, potential trans-BBB treatments of AD in humans.

METHODS

Transgenic mice

Transgenic mice expressing mutant human $APP_{K670N,M671L}$ protein (line Tg2576)22 and a line of mice expressing human mutant $PS1_{M146V}$ protein (line 8.9)23 were crossed to generate off-spring: doubly transgenic APP/PS1 animals and wild-type NTg littermates.24 A total of six mice (age: 12 months, mass: 26−37 g) i.e., transgenic APP/PS1 (n = 3) and NTg (n = 3) mice were used in this study.

Ultrasound methodology

A single-element therapeutic FUS transducer (center frequency: 1.525 MHz, focal depth: 90 mm, radius: 30 mm, Riverside Research Institute, New York, NY, USA) generated ultrasound waves. A pulse-echo diagnostic transducer (center frequency: 7.5 MHz, focal length: 60 mm) was placed through a central, circular hole (radius 11.2 mm) of the FUS transducer so that the foci of the transducers fully intersected (Fig. 1A). A cone filled with degassed and distilled water and sealed with a polyurethane membrane cap (Trojan, Church & Dwight Co., Inc., Princeton, NJ, USA) was mounted onto the transducer. The entire system was attached to a computer-controlled, three-dimensional positioning system (Velmex Inc., Lachine, QC, CAN). The FUS transducer was driven by a function generator (Agilent, Palo Alto, CA, USA) and a 50-dB power amplifier (ENI Inc., Rochester, NY, USA). The pulse-echo transducer was driven by a pulser-receiver system (Panametrics, Waltham, MA, USA), which was connected to a digitizer (Gage Applied Technologies, Inc., Lachine, QC, CAN) integrated into a personal computer (PC, Dell Inc., TX, USA).

The pressure amplitude and three-dimensional beam dimensions of the FUS transducer were measured using a needle hydrophone (Precision Acoustics Ltd., Dorchester, Dorset, UK, needle diameter: 0.2 mm) in a degassed water-tank prior to the *in vivo* experiments. The reported pressure amplitudes were measured by calculating the peak-negative and peak-positive pressure values and attenuating by 18% to correct for murine skull attenuation.18 The lateral and axial full-width-at-half-maximum intensities of the beam were 1.32 and 13.0 mm, respectively.

Sonication protocol

Each mouse was anesthetized using 1.25−2.50% isoflurane (SurgiVet, Smiths Medical PM, Inc., Wisconsin, USA) and its head was immobilized by a stereotaxic apparatus (David Kopf Instruments, Tujunga, CA; Fig. 1). The mouse hair was removed and a degassed water-filled container, sealed at the bottom with an acoustically- and optically-transparent plastic membrane (Saran, SC Johnson, Racine, WI, USA), was placed on the mouse head (Fig. 1A). Ultrasound coupling gel was used to eliminate any remaining impedance mismatch between the skin and the membrane. The FUS transducer was then submerged in the container with its beam axis perpendicular to the surface of the skull.

Using a previously described grid-positioning method, the transducer's beam axis was positioned 2.25 mm and 2 mm away from the sagittal and lambdoid sutures, respectively (Fig. 1B). The focus was placed 3 mm beneath the parietal bone, overlapping with the left hippocampus and the left posterior cerebral artery (PCA). The right hippocampus was not targeted and was used as the control.

A 25 μl bolus of phospholipid-coated sulfur hexafluoride microbubbles (Sono Vue®, Bracco Diagnostics, Inc., Milan, Italy; mean diameter: 3.0−4.5 μm, concentration: $5.0-8.0 \times 10^8$ bubbles per ml) was injected via the tail vein. One minute later, pulsed FUS (pulse rate: 10 Hz, pulse duration: 20 ms, duty cycle: 20%) was applied once in each mouse brain at a peak-

negative pressure of approximately 600 kPa in a series of two 30 s shots of sonication. A 30-s interval between shots allowed for residual heat to dissipate.17

Magnetic resonance imaging protocol

A vertical bore 9.4-Tesla MR system (Bruker Medical, Boston, MA, USA) acquired horizontal slices (matrix size: 256 × 256, field of view: 1.92 × 2.14 cm, slice thickness: 0.6 mm, number of excitations: 5) of the mouse brain in two sessions: MRI scans on day 1 (90 min post-sonication) to depict the BBB opening and MRI scans on day 2 (22 hours post-sonication) to depict the BBB closure. In both sessions, the mice were immobilized in a 3.8-cm-diameter birdcage coil embedded on a plastic tube and inserted into the magnet. 1−2% isoflurane was administered while the respiration rate of the mouse was monitored throughout the procedure. T_2-weighted (Repetition Time / Echo Time [TR/TE]: 4000 ms/9.2 ms, rapid acquisition with relaxation enhancement: 16) and T_1-weighted (TR/TE: 246.1 ms / 10 ms, bandwidth: 50,505.1 Hz) MR sequences were used. Pre-gadolinium T_2-weighted (n = 1, duration: 4 min) and T_1-weighted images (n = 3, duration: 12 min) were acquired to roughly assess any FUS-induced tissue damage and any significant field inhomogeneities between the contralateral hippocampi. A BBB-impermeable, gadolinium-based MRI contrast agent (Omniscan™, Amersham Health, AS Oslo, NOR, amount: 0.75 ml, molecular weight: 573.7 Da) was administered intraperitoneally (IP) via a catheter to depict the BBB opening10 and its spatio-temporal variation.17, 18 IP injection allowed for the slow uptake of the MRI contrast agent into the bloodstream.26 Post-gadolinium sequential T_1-weighted (n = 21, duration: 90 min) and T_2-weighted (n = 1, duration: 4 min) images were then acquired.

Magnetic resonance imaging analysis

T_1-weighted images were processed to (1) identify the contrast-enhanced pixels due to gadolinium deposition, (2) quantify the mean signal intensity (SI) of the striatal and hippocampal regions of interest (ROI) over time, (3) depict the area of contrast-enhancement in the hippocampus over time and (4) depict the spatial variation of the contrast-enhancement levels in the hippocampi at a single time-point. In the first method, the mean SI of a 11×11 pixel (0.825 × 0.920 mm^2) right hippocampus (control) ROI and its standard deviations (SD) were measured. Every pixel of each image was individually subtracted from its mean SI and pixels above 2.5 SD were determined to be contrast-enhanced. The 2.5-SD threshold provided a statistically-significant differentiation between intact and contrast-enhanced regions in all experiments. In the second method, the percentage increase in SI of the left compared to the contralateral right ROI was calculated over 90 min. The mean SI of a 11×11 pixel (0.825 × 0.920 mm^2) ROI of the left and right striata and the left and right hippocampi were each separately measured (Fig. 3A). The normalized increase in SI (S_{norm}) for each region was then calculated:

$$S_{norm} = 100\% \times (SI_{left} - SI_{right}) \quad / \quad SI_{right}$$

where SI_{left} and SI_{right} are the mean SI of the left and right ROIs, respectively. The average and SDs over three experiments were computed. In the third method, spatial color maps depicting the temporal nature of contrast-enhancement were quantified. Any SI above 2.5 SD of the right hippocampus ROI mean SI was determined to be contrast-enhanced. This was repeated at 13, 30, 47, 65 and 82 min post-gadolinium injection, pseudo-colored and overlaid onto the corresponding MR image (Fig. 4). The area of contrast-enhancement was then calculated over time elapsed after gadolinium injection by counting the contrast-enhanced pixels (Fig. 3C). Finally, spatially-varying color maps of contrast-enhancement levels at a single time-point were calculated. For each mouse, the region of contrast-

enhancement 2.5, 5.5, 8.5, 11.5 and 14.5 SDs above the mean SI in the ROI of the right hippocampus was pseudo-colored to distinguish areas of varying gadolinium concentrations (Fig.5). Each color map was then separately overlaid onto its corresponding T_1-weighted image.

Brain preparation and histology

One hour after the final MRI session, each mouse was sacrificed and transcardially perfused with 30 ml of phosphate buffer saline followed by 60 ml of 10% neutral buffered formalin. Its brain was removed, soaked in fixative for 12 hours, embedded in paraffin and horizontally sectioned with a microtome. Sections at 6-μm thick were hematoxylin and eosin (H&E) stained to evaluate macroscopic brain tissue damage while sections at 15-μm thick were thioflavin S stained to confirm the existence of amyloid plaques.

RESULTS

The BBB opening was monitored *in vivo* using a 9.4 T MRI scanner in all mice. MR images were acquired on day 1 (90 min post-sonication) to monitor the BBB opening and day 2 (22 hours post-sonication) to monitor the BBB recovery. No significant MRI SI contrast changes were observed in pre-gadolinium T_1 and T_2-weighted images (Fig. 2), indicating no significant field inhomogeneities and no residual gadolinium (on day 2). Gadolinium deposition through the FUS-induced BBB opening in all transgenic and NTg mice enhanced the SI on T_1-weighted images while suppressing it on T_2-weighted images. Follow-up MRI scans on day 2 depicted significantly reduced T_1-weighted SI enhancement and T_2-weighted SI suppression, indicating possible closure of the BBB. A significant contrast difference between the ROIs in the hippocampi and striata, and between the day-1 and day-2 hippocampi ROIs was observed within the first 43 minutes (Fig. 3B). However, a few pixels in the targeted region exhibited contrast changes on day 2 (Figures 2D, L).

Following gadolinium injection, the cross-sectional area of contrast enhancement increased over time (Fig. 3C). Contrast enhancement began at, or near, the PCA and then gradually expanded into the surrounding regions until it encompassed the entire hippocampus (Fig. 3B). In spite of this, the degree of contrast enhancement was not spatially uniform and regions of local minima and maxima of contrast enhancement were observed throughout the targeted region of each mouse, i.e., there were pixels near the center of the targeted region that were not contrast enhanced (Figs. 5A, C, and E). On day 2, no contrast enhancement in most of the targeted region was observed, most notably in mouse 1 (Figs. 4B, 5B). However, contrast-enhanced pixels remained in the targeted region of mice 2 and 3, especially near the large vessels (i.e., PCA region) (Figs. 4D, F, 5D, F). Regardless, the area of contrast enhancement and the degree of contrast enhancement were significantly reduced on day 2.

Thioflavin-S stained amyloid plaques in the transgenic mice were confirmed (Figs. 6A, B) and compared with NTg mice (Fig. 6C). There were no significant differences in the number of plaques in the left and right hippocampi. Furthermore, no macroscopic damage to the hippocampi was observed when comparing the left to the right hippocampi of the H&E stained sections (Figs. 6D, E).

DISCUSSION

The left hippocampus was accurately targeted through the intact skin and skull in all transgenic APP/PS1 and NTg mice using a previously developed targeting system.18 A single focus using a single-element FUS transducer was sufficient to reproducibly and reliably deposit BBB-impermeable Omniscan™ into the left hippocampus and its surrounding regions (Fig. 2). FUS-induced BBB opening has previously been indicated

through contrast-enhancement of the MRI SI.10, 17, 18 Nevertheless, contrast enhancement could be due to gadolinium traversing openings in the vasculature, diffusing through the interstitial tissue originating from BBB- opened vessels or localization of gadolinium to certain regions of the brain or vasculature. IP injection, as opposed to an IV injection, of gadolinium induces transportation across the peritoneal microvasculature prior to venous transport. Its use allows for a larger amount of injectable gadolinium (0.75 ml), longer temporal analysis of the BBB opening (over 90 min) and reduced mouse mortality and morbidity rates.26 The 90-min MRI scan time was previously determined to be sufficiently long for Omniscan™ to diffuse throughout the hippocampal parenchyma.

Temporal and spatial distributions of gadolinium were analyzed with color maps to facilitate interpretation of all brain images (Figs. 4, 5). Approximately 13 min after gadolinium injection (red region), the contrast-enhanced region extended from the anterior to the posterior regions of the brain and did not exactly have the shape characteristic of the FUS-beam, i.e., a 1.3-mm-diameter circular transverse cross-section.18 This spatial asymmetry at the focal spot was observed, although to a lesser extent, over time. The vessels in the MR images were roughly matched to μCT vascular maps of similar mice to identify them.27 According to these maps, upon IP injection blood diffuses from the PCA to the longitudinal and transverse hippocampal arteries, which perfuse the hippocampi. These vessels are within the FUS-targeted region. Since horizontal slices were obtained, lateral cross-sections of the PCA, or longitudinal hippocampal arteries, were visible with transverse hippocampal arteries assumed to extend laterally clockwise into the hippocampus. Upon IP injection, contrast enhancement was initially detected at the PCA, or longitudinal hippocampal artery and subsequently in the transverse hippocampal arteries, or the region surrounding the hippocampal arteries. At the final time-point (90 min post-gadolinium injection), local minima and maxima in the level of contrast enhancement were observed throughout the sonicated region (Figs. 5A, C, E). These localized, high concentrations of gadolinium were not contiguous along a certain path but were instead dispersed throughout the entire targeted region. A more through study of this phenomenon is currently ongoing.

Partial, or nearly complete, BBB closure was observed in all mice (Figs. 2L, 5B, D, F). BBB recovery was noted in almost the entire targeted region in mouse 1 (Fig. 5B) while mouse 3 (Fig. 5F) experienced the longest time to closure. The BBB recovered at various degrees depending on the targeted location. Regardless, the recoveries in all mice were deemed significant with a low level of contrast enhancement on day 2 (Fig. 3B).

There were no significant differences in the timing and characteristics of the BBB opening between the transgenic (APP/PS1) and NTg mice. However, the BBB recovery varied in some mice (Fig. 2L) and may be due to several reasons. A total of two SonoVue® vials were used multiple times on different days for all six mice. Repeated use of vials may alter the properties of the microbubbles (i.e., bubble radius) due to the leakage of air in the vial from repeated injections to aspirate the mixture. Also, the mouse masses varied and the accuracy of the amount of microbubbles injected (25 μl) was limited by the syringe used. However, the main purpose of this study was to determine the dependence of the FUS-induced BBB opening on the age and disease of the animal model and, based on our measurements, the general behaviors of the two groups of mice were similar.

The long-term goal of this study is to therapeutically target and eliminate, reduce or prevent the formation of the AD plaques. Successful treatment requires a noninvasive, transient, and localized BBB opening, which was demonstrated here in transgenic Alzheimer's-model(APP/PS1) mice. Some of the concerns associated with FUS-induced BBB opening include the opening size, recovery timeline, drug load and safety profile. Normally, the BBB excludes nearly all molecules greater than 400 Da while most neurologically potent

molecules are larger.9 Two categories of potentially disease-modifying drugs that are BBB-impermeable are β-secretase inhibitors and antibodies, which are approximately 1 kDa and 30 to 200 kDa, respectively.28 In this study, a 573.3 Da molecule and, in a separate study, 3 and 70 kDa dextrans were delivered trans-BBB.21 These molecules are larger than most antibodies and, therefore, the size of BBB opening is promising. Previous studies have reported BBB closure within a day of FUS-induced BBB opening with a different microbubble, Optison™.10 However, our study, using different sonication parameters and microbubbles, indicated that this was not always the case in both transgenic and NTg mice. 30 Using high field MRI (9.4 T), BBB recovery varied temporally at different locations of the targeted region. The BBB closure at optimized sonication parameters and carefully engineered microbubbles must be studied in more detail over an extended period of time. The drug load is also critical to a therapeutic study and Treat et al20 have demonstrated the feasibility of delivering doxorubicin HCl liposomes (DOXIL, molecular weight: 579.99 Da), a chemotherapeutic agent, trans-BBB to a clinically-significant level (39% patient response level). Future studies using our technique will evaluate the drug load of delivering either β-secretase or antibodies and the determine the complete safety profile. According to this paper, no macroscopic damage was observed on the H&E sections but a more detailed histological and behavioral analysis must be performed before any final conclusions can be drawn.

Finally, previous studies have shown that the BBB integrity is disrupted in AD-affected human subjects.21 According to the results shown here and based on the limitations of our measurements, there are no significant concerns in AD APP/PS1 mice. The BBB opening in AD mice was found to be insignificantly different from control mice with the opening being transient. The feasibility of delivery of a molecule that normally does not traverse the BBB was hereby shown in APP/PS1 transgenic mice. The next step is to deliver therapeutic agents (i.e., β-secretase) and directly treat AD in the same APP/PS1 transgenic mice using the same ultrasound and targeting techniques.

In summary, an otherwise BBB-impermeable molecule was delivered through the left hippocampal vasculature in one-year-old transgenic APP/PS1 mice. All sonications were applied *in vivo*, after microbubble injection, and through the intact skin and skull of the mouse using a single sonication generated by a single-element transducer. Although the distribution of the gadolinium was not entirely uniform, it permeated the entire targeted hippocampal region. Also, the opening was observed to be transient with recovery observed within a day in some cases. To our knowledge, this is the first demonstration of a noninvasive, transient and localized delivery of an otherwise BBB-impermeable molecule in a disease-model animal.

Acknowledgments

The authors thank the Riverside Research Institute for providing the transducers; Barclay Morrison III, Ph.D. (Department of Biomedical Engineering, Columbia University) for several fruitful discussions; Sujan Doshi and Kristen Kim for assistance with the *in vivo* mouse experiments; Abhiraj Modi for developing the graphical user interface for the targeting and sonication procedures and assistance with performing the *in vivo* mouse experiments. This study was supported by NIH R21 EY018505 and NSF CAREER 0644713.

REFERENCES

1. Wimo A, Winblad B, Aguero-Torres H, von Strauss E. The magnitude of dementia occurrence in the world. Alzheimer Disease Assoc Disorders. 2003; 17:63–7.
2. Hull M, Berger M, Heneka M. Disease-modifying therapies in Alzheimer's disease: how far have we come? Drugs. 2006; 66:2075–2093. [PubMed: 17112302]

3. Areosa SA, Sherriff F, McShane R. Memantine for dementia. Cochrane Database Systematic Rev (Online). 2005:CD003154.
4. Birks J, Harvey RJ. Donepezil for dementia due to Alzheimer's disease. Cochrane Database Systematic Rev (Online). 2006:CD001190.
5. Pardridge WM. The blood-brain barrier: bottleneck in brain drug development. NeuroRx. 2005; 2:3–14. [PubMed: 15717053]
6. Hills ID, Vacca JP. Progress toward a practical BACE-1 inhibitor. Current Opinion Drug Discovery Develop. 2007; 10:383–391.
7. Barten DM, Meredith JE Jr. Zaczek R, Houston JG, Albright CF. Gamma-secretase inhibitors for Alzheimer's disease: balancing efficacy and toxicity. Drugs R&D. 2006; 7:87–97.
8. Stewart PA, Tuor UI. Blood-eye barriers in the rat: correlation of ultrastructure with function. J Comp Neurol. 1994; 340:566–576. [PubMed: 8006217]
9. Pardridge WM. Drug targeting to the brain. Pharma Res. 2007; 24:1733–1744.
10. Hynynen K, McDannold N, Vykhodtseva N, Jolesz FA. Noninvasive MR imaging-guided focal opening of the blood-brain barrier in rabbits. Radiology. 2001; 220:640–646. [PubMed: 11526261]
11. Reinhard M, Hetzel A, Kruger S, et al. Blood-brain barrier disruption by low-frequency ultra sound. Stroke. 2006; 37:1546–1548. [PubMed: 16645131]
12. McDannold N, Vykhodtseva N, Hynynen K. Targeted disruption of the blood-brain barrier with focused ultrasound: association with cavitation activity. Phys Med Biol. 2006; 51:793–807. [PubMed: 16467579]
13. Kinoshita M, McDannold N, Jolesz FA, Hynynen K. Noninvasive localized delivery of Herceptin to the mouse brain by MRI-guided focused ultrasound-induced blood-brain barrier disruption. Proc Natl Acad Sci. 2006; 103:11719–11723. [PubMed: 16868082]
14. Choi, JJ.; Pernot, M.; Small, SA.; Konofagou, EE. Proc IEEE Ultrason Symp. IEEE; 2005. Feasibility of transcranial, localized drug-delivery in the brain of Alzheimer's-model mice using focused ultrasound; p. 988-999.
15. Choi JJ, Pernot M, Small S, Konofagou EE. Noninvasive Blood-Brain Barrier Opening in Live Mice. AIP Proc. 2006; 829:271–275.
16. Choi, JJ.; Small, SA.; Konofagou, EE. Proc IEEE Ultrason Symp. IEEE; 2006. Optimization of blood-brain barrier opening in mice using focused ultrasound; p. 540-543.
17. Choi JJ, Pernot M, Brown TR, Small SA, Konofagou EE. Spatio-temporal analysis of molecular delivery through the blood-brain barrier using focused ultrasound. Phys Med Biol. 2007; 52:5509–5530. [PubMed: 17804879]
18. Choi JJ, Pernot M, Small SA, Konofagou EE. Noninvasive, transcranial and localized opening of the blood-brain barrier using focused ultrasound in mice. Ultrasound Med Biol. 2007; 33:95–104. [PubMed: 17189051]
19. Raymond SB, Skoch J, Hynynen K, Bacskai BJ. Multiphoton imaging of ultrasound/Optison mediated cerebrovascular effects in vivo. J Cereb Flow Metab. 2007; 27:393–403.
20. Treat LH, McDannold N, Vykhodtseva N, et al. Targeted delivery of doxorubicin to the rat brain at therapeutic levels using MRI-guided focused ultrasound. Int J J Cancer. 2007; 121:901–907.
21. Choi, JJ.; Wang, S.; Morrison, B., III; Konofagou, EE. Proc IEEE Ultrason Symp. IEEE; 2007. Molecular delivery and microbubble dependence study of the FUS-induced blood-brain barrier opening in vivo; p. 1192-1195.
22. Hsiao K, Chapman P, Nilsen SE, et al. Correlative memory deficits, Abeta elevation, and amyloid plaques in transgenic mice. Science. 1996; 274:99–102. [PubMed: 8810256]
23. Duff K, Eckman C, Zehr C, et al. Increased amyloid-beta42(43) in brains of mice expressing mutant presenilin 1. Nature. 1996; 383:710–713. [PubMed: 8878479]
24. McGowan E, Sanders S, Iwatsubo T, et al. Amyloid phenotype characterization of transgenic mice overexpressing both mutant amyloid precursor protein and mutant presenilin 1 transgenes. Neurobiol Disease. 1999; 6:231–244.
25. Ford JC, Wood AK, Van Winkle TJ, Kundel HL. Magnetic resonance imaging observations of blood-brain-barrier permeability in an animal model of brain injury. Acad Radiol. 1997; 4:115–126. [PubMed: 9061084]

26. Moreno H, Hua F, Brown T, Small S. Longitudinal mapping of mouse cerebral blood volume with MRI. NMR Biomed. 2006; 19:535–43. [PubMed: 16552789]

27. Dorr A, Sled JG, Kabani N. Three-dimensional cerebral vasculature of the CBA mouse brain: a magnetic resonance imaging and micro computed tomography study. NeuroImage. 2007; 35:1409–1423. [PubMed: 17369055]

28. Jain M, Kamal N, Batra SK. Engineering antibodies for clinical applications. Trends Biotech. 2007; 25:307–316.

29. Algotsson A, Winblad B. The integrity of the blood-brain barrier in Alzheimer's disease. Acta Neurol Scand. 2007; 115:403–8. [PubMed: 17511849]

30. Konofagou, EE.; Choi, JJ. Ultrasound-induced treatment of neurodegenerative diseases across the blood-brain barrier,in Biomedical Applications of Vibration and Acoustics in Therapy. In: Al-Jumaily, A.; Fatemi, M., editors. Bioeffects and Modelling. ASME Press; 2008. p. 63-80.

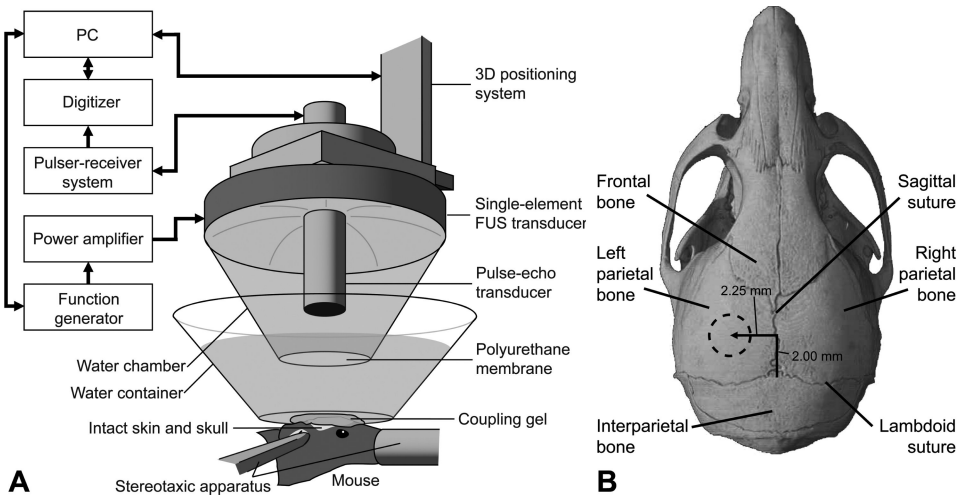

FIG. 1.

(A) Experimental set-up. The focal region of the FUS transducer was positioned through (B) the left parietal bone of the mouse skull (dotted circle in (B)) to target the left hippocampus.

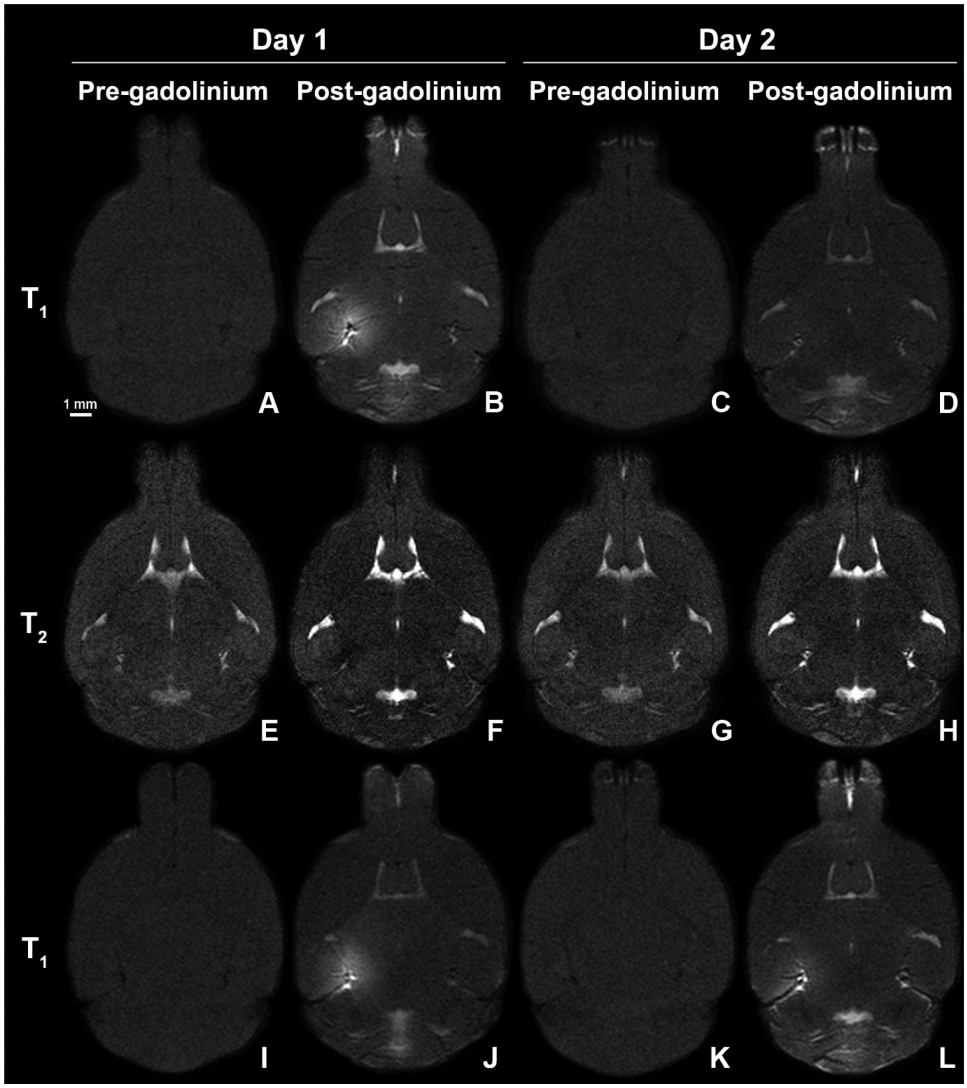

FIG. 2.

T_1-weighted and T_2-weighted MR images of a transgenic (A-H) and NTg (I-L) mouse brain after FUS-induced BBB opening acquired on day 1 before (A, E, I) and 90 min after (B, F, J) gadolinium injection. On day 2, a second series of MR images were acquired before (C, G, K) and 90 min after (D, H, L) a second dosage of gadolinium injection. Contrast changes were observed on day 1 while less to no change was observed on day 2.

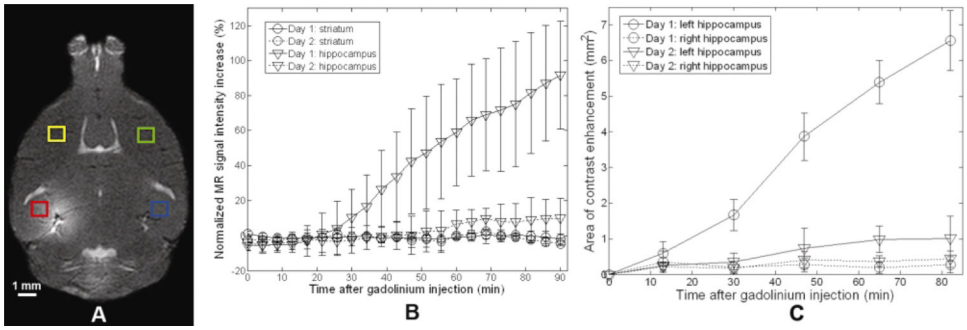

FIG. 3.

(A) MRI contrast changes in the left (red, FUS-targeted) and right (blue, control) hippocampus, and the left (yellow) and right (green) striatum ROIs were monitored. (B) Mean SI was calculated over time in the striatum (circles) and the hippocampus (triangles) regions and significant contrast enhancement of the left hippocampus was observed on day 1 (solid) with less contrast enhancement observed on day 2 (dashed), indicating partial closing of the BBB. (C) Cross-sectional area of contrast enhancement of the left (targeted) and right (control) hippocampi after gadolinium injection in transgenic APP/PS1 mice was monitored. Data were extracted from two MRI scans obtained on day 1 (circle) and day 2 (triangle).

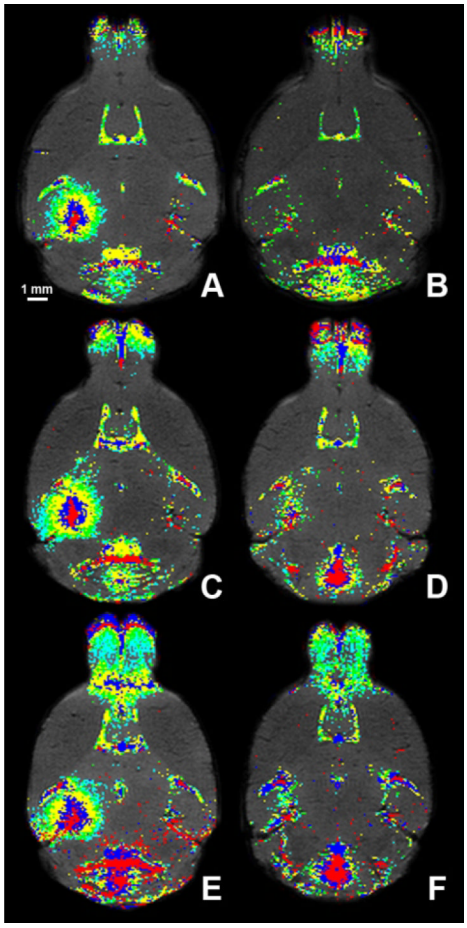

FIG. 4.

In vivo spatio-temporal maps of the FUS-induced BBB opening on day 1 (A, C, E) and day 2 (B, D, F) in three APP/PS1 mice. The first (A, B), second (C, D), and third (E, F) mouse brains were analyzed with sequential T1–weighted images that depicted the slow diffusion of gadolinium 13 min (red), 30 min (blue), 47 min (yellow), 65 min (green) and 82 min (cyan) after its intraperitoneal injection.

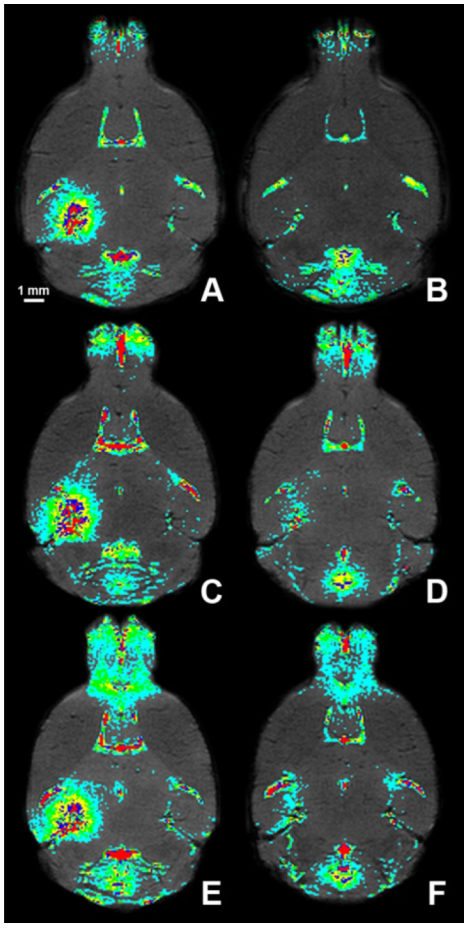

FIG. 5.

In vivo spatial maps of the FUS-induced BBB opening on day 1 (A, C, E) and (B, D, F) day 2 (B, D, F). The first (A, B), second (C, D) and third (E, F) mouse brains were analyzed 90 min post-gadolinium injection using T_1-weighted MRI. Regions of contrast enhancement above 2.5 (cyan), 5.5 (green), 8.5 (yellow), 11.5 (blue) and 14.5 (red) standard deviations above the mean signal intensity of the control (right) hippocampal region of interest were highlighted.

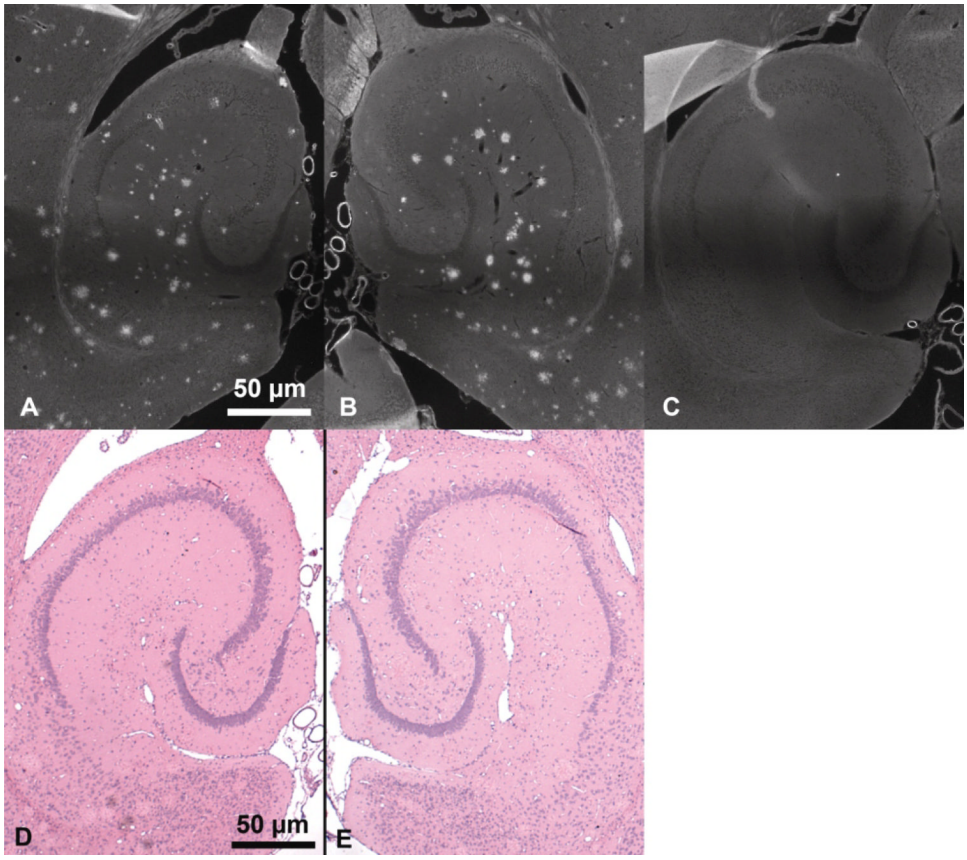

FIG. 6.

Thioflavin-S histologic sections of the sonicated left (A) and control right (B) hippocampi of transgenic APP/PS1 mice and the left hippocampus of a control (C) mouse. The dark, diffuse band across each image is an artifact due to stitching several images together. Hematoxylin and eosin histologic sections of the left (D) and right (E) hippocampi of a transgenic APP/PS1 mouse.